Record High Conversion Gain Ambipolar Graphene Mixer at 10GHz Using Scaled Gate Oxide

H. Madan, M. J. Hollander, M. LaBella, R. Cavalero, D. Snyder, J. A. Robinson, and S. Datta
The Pennsylvania State University, University Park, Pennsylvania 16802, United States
Tel: (814) 689-9483, Fax: (814) 865-7065, Email: himanshu@psu.edu

Abstract

This work presents a detailed study of the graphene RF mixer, comparing ambipolar and drain mixing for the first time. Output characteristics of the graphene transistor are analyzed and the effects of device scaling and interface state density on mixer performance are explained. We design a graphene RF transistor with gate length 750 nm, width 20 µm, and equivalent oxide thickness (EOT) ~2.5 nm to achieve record high conversion gain of -14 and -16 dB at LO power 0 dBm at 4.2 and 10 GHz, respectively, 100x higher than previously reported ambipolar mixing.

Introduction

In recent years, graphene has gained interest for use in RF electronic devices due to its high carrier mobility, symmetric electron and hole conduction, and ambipolar behavior. These unique properties have allowed for novel RF applications, including a single transistor triple-mode amplifier [1] and a single transistor ambipolar mixer [2]. For the second case, graphene's ambipolar nature (Fig. 1a) allows for suppression of odd order harmonics at the Dirac point as well as peak conversion gain, where small signal output at the drain is given as:

$$i_{ds} = g_m v_{gs} + g'_m v_{gs}/2 + g''_m v_{gs}/6 + \ldots$$

Suppression of odd order harmonics is a result of g_m and g''_m both vanishing at the Dirac point, while g'_m experiences a maximum (Fig. 1b). Additionally, more conventional mixer designs have also been implemented showing resistive [3] and drain mixing [4]. Although initial demonstrations have been successful, performance has been limited by high contact resistance, low mobility, and low transconductance. By analyzing the DC/RF output characteristics of the graphene transistor, we identify the key areas to improve mixer performance, leading to record high conversion gain.

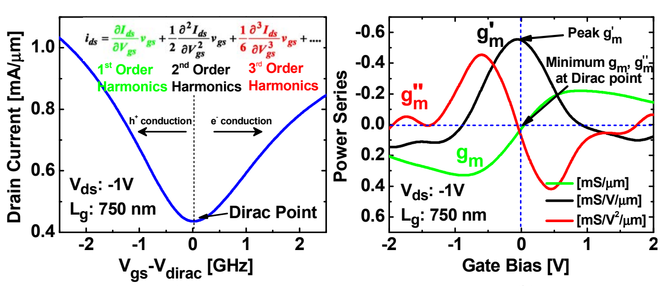

(a) (b)

Figure 1. Ambipolar conduction leads to high conversion gain and suppression of odd order mixing products at transistor output. (a) Transfer curve of graphene FET showing ambipolar behavior. (b) Extracted first, second, and third order components of drain current showing peak g'_m as well as minimum g_m and g''_m at the Dirac point.

Synthesis, Materials, and Fabrication

Graphene is prepared on (0001) oriented, semi-insulating 6H-SiC through combination of sublimation and hydrogen intercalation leading to carrier mobilities as high as 3000 $cm^2/V\cdot sec$ at 10^{13} cm^{-2}. Sublimation of Si takes place at 1625°C in 1 Torr Ar, while hydrogen intercalation follows at 1050°C in 600 Torr Ar/H_2, producing primarily bilayer graphene across the hydrogen passivated SiC surface. Hydrogen intercalation is a key step in maintaining high carrier mobility for epitaxial graphene. Graphene transistors were patterned using standard photolithographic techniques (Fig. 2). Source/drain contacts were deposited with a pre-metallization oxygen de-scum [5] to achieve contact resistances as low as 100 ohm-µm. Gate dielectrics were deposited using an EBPVD seeded ALD process (10 nm HfO_2) discussed elsewhere [6]. For the gate dielectric, use of the two-step EBPVD seeded ALD process allows for scaling the EOT to ~2.5 nm while maintaining uniform coverage and without significantly degrading transport properties.

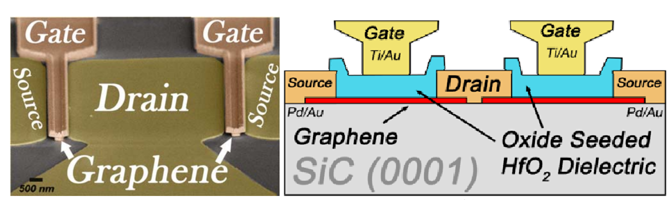

(a) (b)

Figure 2. (a) False color SEM micrograph of two-finger graphene RF transistor with T-gates. (b) Schematic cross-section of graphene transistor with L_g=750nm and W=20µm. 10nm HfO_2 gate oxide was grown by oxide seeded ALD as described elsewhere [6].

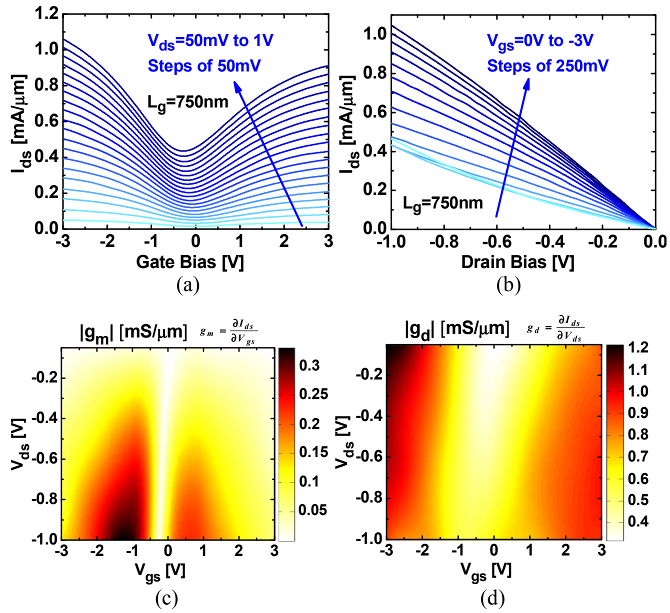

Figure 3. (a) Transfer curves (I_{ds}-V_{gs}) from V_{ds}=50mV to 1V exhibiting V_{Dirac} near V_{gs}=0V and near symmetric electron and hole branches. (b) Family of curves (I_{ds}-V_{ds}) from V_{gs}=0 to -3V showing weak saturation behavior. (c),(d) Color maps of absolute transconductance (g_m) and output conductance (g_d) as a function of drain bias (V_{ds}) and gate bias (V_{gs}) indicating a peak transconductance of 330 μS/μm.

Graphene FET Performance

DC characteristics of HfO_2 gated transistors display on-off ratios >2 and demonstrate excellent drive current of 1.1 mA/μm at V_{ds}= -1V (Fig. 3a,b). Peak transconductance is found to be 330 μS/μm (Fig. 3c), which is attributed to the relatively small EOT for these devices (~2.5 nm) as well as the high mobility of the hydrogen passivated epitaxial graphene. RF performance is excellent, exhibiting peak intrinsic current gain cutoff frequency (f_T) of 110 GHz at a gate length of 75 nm with V_{ds}= -1V, where intrinsic f_T was extracted from measured S-parameters using a standard short-open de-embed process to remove the effect of probe and pad parasitics. Intrinsic f_T is found proportional to the inverse of L_g, although extrinsic performance is limited by parasitics at small gate lengths. Still, we report an excellent peak extrinsic $f_T{\cdot}L_g$ ~5 GHz·μm (Fig. 4b). Effective injection velocity between 1.1 and 2.5x10^7 cm/sec (Fig. 4d) is extracted from the small signal parameters as a function of L_g. Third-order intermodulation is characterized using two-tone measurements at 4 and 4.2 GHz, giving a third-order intermodulation intercept (TOI) of 17.5 dBm. (Fig. 5a). TOI as a function of DC dissipated power shows that graphene devices are competitive with conventional semiconductor devices (Fig. 5b).

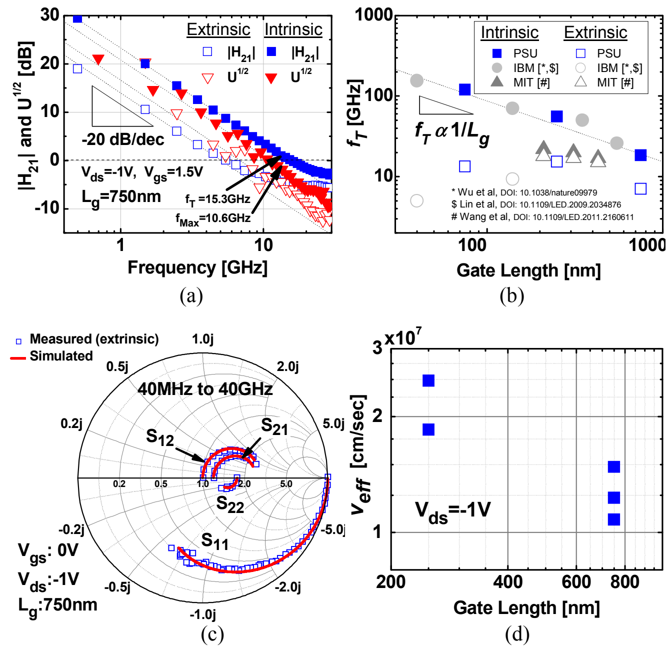

Figure 4. (a) Short circuit current gain and unilateral power gain of graphene transistor at V_{ds}=-1V and V_{gs}=1.5V. Intrinsic values are extracted using a short-open de-embed process in order to remove probe and pad parasitics. (b) Intrinsic and extrinsic f_T as a function of gate length, showing increasing effect of parasitics on extrinsic device performance as well as the expected dependency of f_T on L_g. (c) Measured and simulated S-parameters for L_g=750nm device showing excellent fit. (d) Extracted effective velocity as a function of gate length.

Mixer Performance

Ambipolar mixing is achieved through gate mixing of the LO and RF input signals (Fig. 6a). The LO and RF inputs of 4.2 (10) and 4 (9.8) GHz, respectively, were combined using an external power combiner. A plot of g_m' versus V_{gs} and V_{ds} identifies the Dirac point as the optimal bias point for maximum conversion gain (Fig. 6b) due to the fact that $P_{IF} \propto g_m'$. Fig. 5c shows the output spectrum at the Dirac point for LO power 0 dBm and RF power -15 dBm, displaying record conversion gain of -14 (-16) dB. Mixer performance was eva-

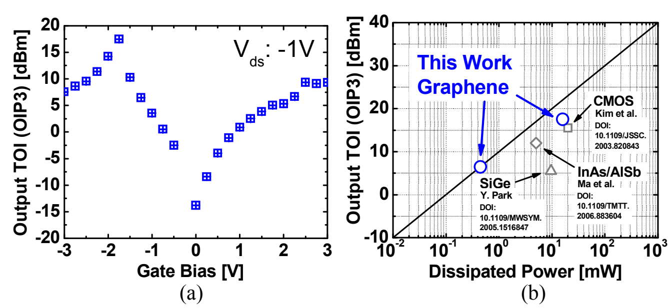

Figure 5. Graphene transistors exhibit excellent linearity compared to conventional transistors. (a) Plot showing the dependency of the third order intercept on gate bias. (b) TOI versus DC dissipated power, showing graphene FET approaching (OIP3>10*Dissipated Power).

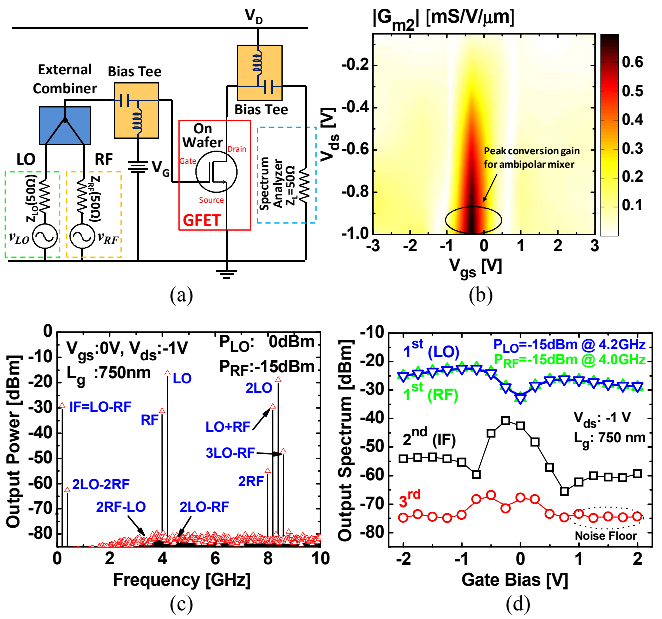

Figure 6. Peak conversion gain is achieved using ambipolar mixing at the gate terminal. (a) Measurement setup for ambipolar graphene mixer. (b) Measured g'_m ($P_{IF} \propto g'_m$) as function of V_{gs} and V_{ds} shows peak g'_m and indicates that maximum conversion gain should occur at the Dirac point. (c) Output spectrum for graphene ambipolar mixer, showing first, second, and third order mixing products as well as record high conversion gain of -14 dB at LO 0 dBm. (d) Measured output spectrum as a function of V_{gs} shows suppression of odd order harmonics and confirms peak conversion gain at the Dirac point.

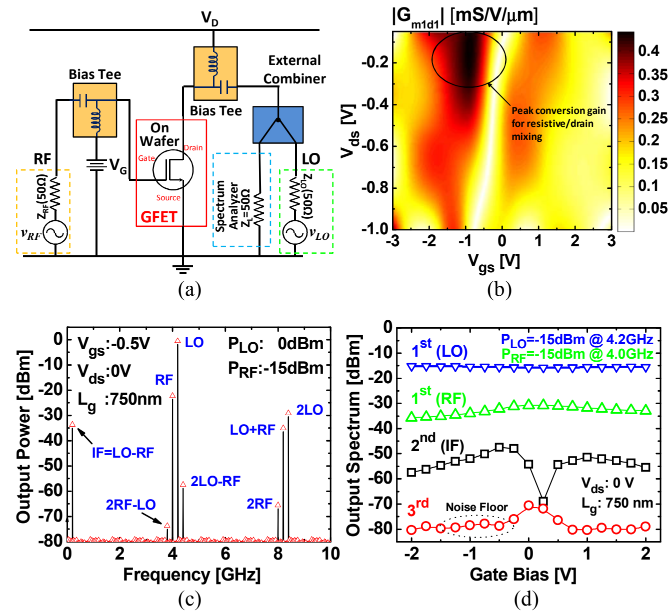

Figure 7. Resistive drain mixing is an alternative to ambipolar gate mixing, but does not suppress odd ordered harmonics. (a) Measurement setup. (b) Measured $g_m g_d$ ($P_{IF} \propto g_m g_d$) as function of V_{gs} and V_{gd} indicating peak values near V_{ds}=0V, thus resistive mixing with V_{ds}=0V should produce the highest conversion gain. (c) Output spectrum for graphene mixer, showing first, second, and third order mixing products and conversion gain of -18.5dB. (d) Measured output spectrum at V_{ds}=0V as a function of V_{gs}, showing no suppression of odd order output products as occurs for the ambipolar gate mixing case.

luated as a function of gate bias showing suppression of odd order harmonics at the Dirac point as well as confirming peak conversion gain at the Dirac point. As a comparison, drain mixing was also considered (Fig. 7a), where:

$$i_{ds} = g_m v_{gs} + g_d v_{ds} + g_m g_d v_{gs} v_{ds} + \ldots$$

A plot of $g_m g_d$ $(= \partial^2 I_{ds} / \partial V_{gs} \partial V_{ds})$ versus V_{gs} and V_{ds} identifies V_{ds}=0V as the optimal bias conditions for drain mixing (resistive mixing) due to the fact that $P_{IF} \propto g_m g_d$ (Fig. 7b). A conversion gain of -18.5 dB is observed at LO power 0 dBm at 4.2GHz and RF at 4 GHz (Fig. 7c), while a sweep in V_{gs} confirms the lack of suppression of odd order harmonics (Fig. 7d).

The effect of interface state density (D_{it}) and scaled EOT were also considered. Fig. 8a shows the effect of increased D_{it} on the transfer characteristics (I_{ds}-V_{gs}), leading to spread in the V-shaped output and, subsequently, reduction in g'_m as well as. $g_m g_d$ Conversion gain is improved by reducing D_{it} or, alternatively, by scaling EOT to smaller thicknesses (Fig. 8b).

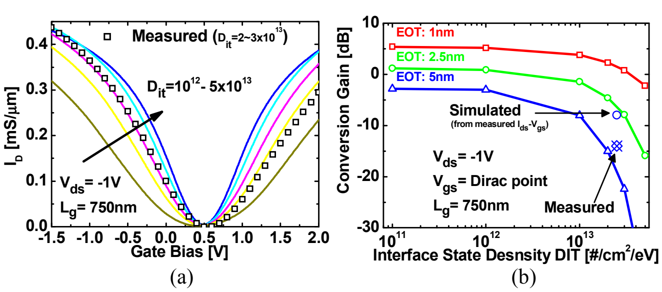

Figure 8. Reduction of interface states and EOT can lead to improved conversion gain. (a) Effect of D_{it} on transfer characteristics of graphene transistor showing spread in the V-shaped output and, subsequently, reduction in g'_m and $g_m g_d$. (b) Plot of conversion gain versus D_{it} for three separate values of EOT (simulation does not account for parasitics).

Benchmark

Conversion gain as a function of LO power shows linear performance up to 0 dBm for both ambipolar and resistive drain mixing (Fig. 9). This work represents the highest performance graphene based mixer yet reported and, furthermore, utilizes the smallest physical width (20μm) of all reported graphene mixers, where increased width is expected to show increased conversion gain. The excellent performance is attributed to highly scaled EOT, high mobility, and low contact resistances (Table 1).

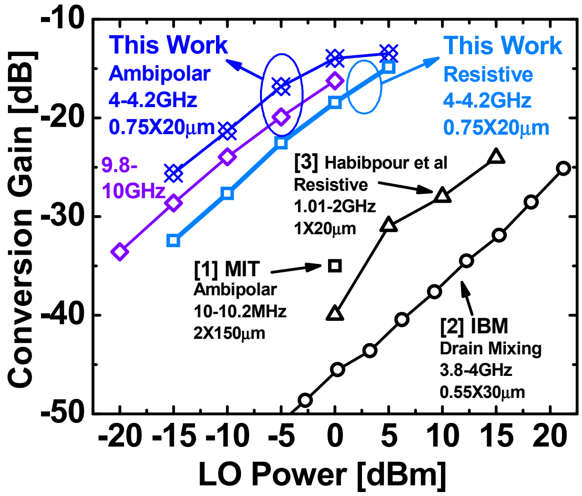

(a)

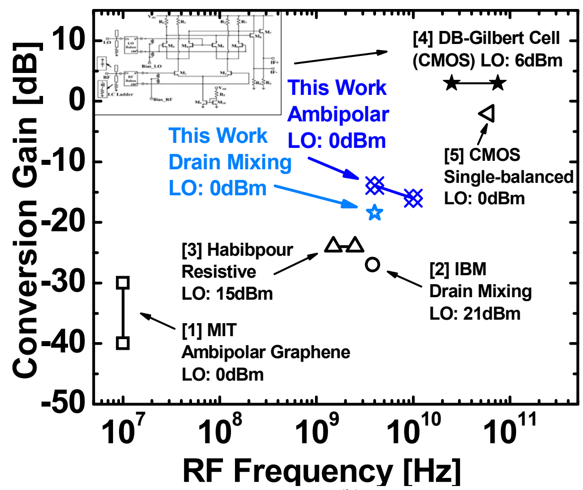

(b)

Figure 9. Record high conversion gain of -14dB for graphene based device at 4GHz demonstrated using ambipolar gate mixing and gate width of only 20µm. (a) Conversion gain versus LO power showing higher conversion gain for ambipolar gate mixing as compared to resistive drain mixing. (b) Conversion gain versus frequency showing operation up to 10GHz. High frequency and high gain mixer performance in this work is attributed to highly scaled EOT, high mobility, and low contact resistance compared to other graphene based mixers (Table 1).

TABLE I
Conversion gain benchmark parameters

Reference	# of FETs	L_g [µm]	W [µm]	t_{ox} [seed/oxide nm]	Peak g_m [µS/µm]	V_{gs} [V]	V_{ds} [V]	R_{con} [Ω·µm]
This Work (Ambipolar)	1	0.75	20	2/10 (HfO_2)	330	0	-1	100
This Work (Resist/Drain)	1	0.75	20	2/10 (HfO_2)	330	-0.5	0	100
[1] Wang et al, DOI: 10.1109/LED.2010.2052017	1	2.0	150	5/25 (SiO_2/Al_2O_3)	5.5	-0.2	--	2-5k
[2] Lin et al, DOI: 10.1126/science.1204428	1	0.55	30	2/20 (Al_2O_3)	80	-3	2	600
[3] Habibpour et al, DOI: 10.1109/LED.2011.2170655	1	1	20	2/25 (Al_2O_3)	35[0.1V]	1	0	560
[4] Tsai et al, DOI: 10.1109/LMWC.2007.892934	10	--	--	--	--	--	--	--
[5] Emami et al, DOI: 10.1109/RFIC.2005.1489619	2	0.13	80	--	--	--	--	--

Conclusions

In conclusion, hydrogen intercalated graphene transistors with highly scaled EOT were used to demonstrate record high conversion gain for a single graphene transistor ambipolar mixer, achieving a small circuit footprint. Ambipolar gate mixing was shown to suppress odd order harmonics and was found to outperform resistive drain mixing. Increased performance is anticipated through further reducing D_{it} and scaling EOT, indicating that the graphene based ambipolar mixer may soon become competitive with conventional Gilbert cell mixers.

Acknowledgement

We acknowledge financial support from Office of Naval Research (ONR).

References

[1] X. Yang, G. Liu, A. A. Balandin and K. Mohanram, "Triple-Mode Single-Transistor Graphene Amplifier and Its Applications," *ACS Nano,* vol. 4, pp. 5532-5538, 2010.

[2] H. Wang, A. Hsu, J. Wu, J. Kong and T. Palacios, "Graphene-Based Ambipolar RF Mixers," *Electron Device Letters, IEEE,* vol. 31, pp. 906 -908, sept. 2010.

[3] O. Habibpour, S. Cherednichenko, J. Vukusic, K. Yhland and J. Stake, "A Subharmonic Graphene FET Mixer," *IEEE Electron Device Letters,* vol. 33, pp. 71-73, jan 2012.

[4] Y.-M. Lin, A. Valdes-Garcia, S.-J. Han, D. B. Farmer, I. Meric, Y. Sun, Y. Wu, C. Dimitrakopoulos, A. Grill, P. Avouris and K. A. Jenkins, "Wafer-Scale Graphene Integrated Circuit," *Science,* vol. 332, pp. 1294-1297, 2011.

[5] J. A. Robinson, M. LaBella, M. Zhu, M. Hollander, R. Kasarda, Z. Hughes, K. Trumbull, R. Cavalero and D. Snyder, "Contacting graphene," *Applied Physics Letters,* vol. 98, p. 053103, 2011.

[6] M. J. Hollander, M. LaBella, Z. R. Hughes, M. Zhu, K. A. Trumbull, R. Cavalero, D. W. Snyder, X. Wang, E. Hwang, S. Datta and J. A. Robinson, "Enhanced Transport and Transistor Performance with Oxide Seeded High-κ Gate Dielectrics on Wafer-Scale Epitaxial Graphene," *Nano Letters,* vol. 11, pp. 3601-3607, 2011.